7th International Conference on Multiphase Flow,
ICMF 2010, Tampa, FL, May 30 – June 4, 2010

Modeling the Random Uncorrelated Velocity Stress Tensor for Unsteady Particle Eulerian Simulation in Turbulent Flows

E. Masi*‡, E. Riber†, P. Sierra†, O. Simonin*‡, L.Y.M. Gicquel†

* Université de Toulouse; INPT, UPS; IMFT; Allée Camille Soula, F-31400 Toulouse, France

‡ CNRS; Institut de Mécanique des Fluides de Toulouse; F-31400 Toulouse, France

† CERFACS; 42, avenue Gaspard Coriolis, F-31057 Toulouse Cedex 01, France

masi@imft.fr, simonin@imft.fr

Keywords: particle-laden flows, Eulerian modeling, one-point closure, axisymmetric state

Abstract

In the Eulerian framework, the dispersed phase of a particle-laden turbulent flow may be modeled by using a statistical approach known as the mesoscopic Eulerian formalism (Février *et al.*, 2005). At the first order, the evolution of the first moments of the conditional probability distribution function, namely the mesoscopic particle number density and the mesoscopic particle velocity, supply the description of the dispersed phase, and the second-order moment appearing in the momentum equation, accounting for the momentum transport due to the particle random uncorrelated velocity, needs to be modeled. In literature, in order to close this moment, referred to as RUM stress tensor, an additional transport equation for the spherical part of the tensor, including the RUM kinetic energy, has been used and a viscosity model for the deviatoric RUM has been suggested (Simonin *et al.* 2002). The latter when *a priori* (Moreau 2006) and *a posteriori* (Kaufmann *et al.* 2008, Riber 2007) tested gives quite satisfactory results in particle-laden homogeneous isotropic turbulence but it fails when performing preliminary *a posteriori* tests (Riber 2007) in mean-sheared turbulent particle-laden flows (Hishida 1987).
In this paper, the concern of the adequacy of such a model for predicting uncorrelated stresses is addressed. An analysis of the tensor structure will make it possible to supply an alternative modeling less sensitive to the change of the particle inertia. The new models are *a priori* checked over several simulations varying in Stokes number; *a posteriori* tests are ongoing.

Nomenclature

Symbols

$\widetilde{g}$	mesocopic quantities
δg	RUM quantities
$\mathbf{G}$	second-rank tensors
$\mathbf{G}^*$	Traceless tensor

Introduction

Février, Simonin & Squires (2005) suggested a statistical approach, known as the mesoscopic Eulerian formalism (MEF), able to describe the local and instantaneous behavior of particles interacting with unsteady and inhomogeneous turbulent flows. Eulerian quantities are defined as the moments of the one-point conditional probability distribution function (p.d.f.) associated to one-fluid flow realization. The Eulerian local and instantaneous transport equations are then obtained in the general frame of the kinetic theory of dilute gases, namely by integration over the particle-velocity space of a Boltzmann-like equation (Reeks 1991). Such an approach consists in partitioning the particle velocity into two contributions: i) an Eulerian particle velocity field referred to as "mesoscopic" which is a continuous field shared by all the particles and accounting for correlations between particles and between particles and fluid; ii) a random spatially-uncorrelated contribution, associated with each particle and satisfying the molecular-chaos assumption. It is referred to as "RUM" (Random Uncorrelated Motion) and it is characterized in terms of Eulerian fields of particle-velocity moments. The originality of this formalism is to make it possible to separate contributions which are intrinsically different, which do not interact in the same way with the different scales of

the turbulence and thus should be modeled in their own way.

At the first order, in isothermal condition, the dispersed phase is fully described by the evolution of the mesoscopic particle number density and the mesoscopic particle velocity as follows (Février *et al.* 2005):

$$\frac{\partial \tilde{n}_p}{\partial t} + \frac{\partial \tilde{n}_p \tilde{u}_{p,i}}{\partial x_i} = 0 \quad (1)$$

$$\frac{\partial \tilde{n}_p \tilde{u}_{p,i}}{\partial t} + \frac{\partial \tilde{n}_p \tilde{u}_{p,i} \tilde{u}_{p,j}}{\partial x_j} = -\frac{\tilde{n}_p}{\tilde{\tau}_p}\left(\tilde{u}_{p,i} - u_{f,i}\right) - \frac{\partial \tilde{n}_p \delta R_{p,ij}}{\partial x_j}. \quad (2)$$

The first term on the right hand side (r.h.s.) of Eq. (2) represents the momentum transfer through the drag force while the second term is the momentum transport due to the particle uncorrelated velocity contribution. The RUM tensor $\delta R_{p,ij}$ may be considered as equivalent to the stress tensor accounting for in the Navier-Stokes (NS) equations, similarly derived by using the Boltzmann kinetic theory. The RUM is composed of a spherical part including the RUM kinetic energy $\delta\theta_p$ which corresponds to the translation temperature in kinetic theory of dilute gases, and a deviatoric part $\delta R^*_{p,ij}$ which is analogous to the viscous contribution due to the thermal agitation in the NS equations:

$$\delta R_{p,ij} = \delta R^*_{p,ij} + \frac{1}{3}\delta R_{p,kk}\delta_{ij} = \delta R^*_{p,ij} + \frac{2}{3}\delta\theta_p\delta_{ij}. \quad (3)$$

The RUM kinetic energy is generally obtained by an additional closed transport equation (e.g., see Kaufmann *et al.* 2008) and only the deviatoric RUM needs to be modeled. The latter is the topic of the present study.

State of the art

In literature, only one model has been suggested in order to close the unknown deviatoric RUM (Simonin *et al.* 2002). This model was *a priori* (Moreau 2006) and *a posteriori* (Kaufmann *et al.* 2008, Riber 2007) tested in homogeneous isotropic turbulence showing quite satisfactory results for moderate Stokes numbers. Instead, such a model strongly fails (Riber 2007) when performing preliminary *a posteriori* tests in mean-sheared turbulent particle-laden flows (Hishida 1987). Comparisons with experiments showed a re-laminarization of the dispersed phase: the particle mesoscopic fluctuations were considerably damped and only the RUM contributed to the particle agitation.

In this work the concern of the adequacy of such a model to predict the second-order moment is addressed.

The viscosity model is here recalled:

$$\delta R^*_{p,ij} = -2\nu_t S^*_{p,ij} \quad (4)$$

where $\nu_t = \frac{\tilde{\tau}_p}{3}\delta\theta_p$ is the so-called mesoscopic viscosity, $\tilde{\tau}_p$ is the mesoscopic particle relaxation time and

$$S^*_{p,ij} = \frac{1}{2}\left(\frac{\partial \tilde{u}_{p,i}}{\partial x_j} + \frac{\partial \tilde{u}_{p,j}}{\partial x_i} - \frac{2}{3}\frac{\partial \tilde{u}_{p,m}}{\partial x_m}\delta_{ij}\right) \quad (5)$$

is the deviatoric symmetric part of the mesoscopic velocity-gradient tensor accounting for shearing or distortion of any element of the dispersed phase. The viscosity model, hereinafter referred to as "VISCO", may be obtained from the second-order moment transport equation:

$$\tilde{n}_p \frac{D}{Dt}\delta R_{p,ij} = -\tilde{n}_p \delta R_{p,kj}\frac{\partial \tilde{u}_{p,i}}{\partial x_k} - \tilde{n}_p \delta R_{p,ik}\frac{\partial \tilde{u}_{p,j}}{\partial x_k} - 2\frac{\tilde{n}_p}{\tilde{\tau}_p}\delta R_{p,ij} - \frac{\partial}{\partial x_k}\tilde{n}_p \delta Q_{p,ijk} \quad (6)$$

assuming equilibrium, i.e. neglecting all the transport terms, and light anisotropy.

The assumptions of both equilibrium and light anisotropy revealed wrong especially in presence of a mean-shear and when increasing inertia. Results of *a priori* testing will confirm the inadequacy of such a model to predict deviatoric RUM stresses.

Numerical simulations

In order to *a priori* test the model in presence of a mean shear, a configuration corresponding to a particle-laden turbulent planar jet is chosen. Direct numerical simulations of the turbulence, one-way coupled with Lagrangian tracking of particles, were performed. Several simulations varying in particle inertia were carried out. Lagrangian values were then post-processed and "exact" Eulerian mesoscopic fields were computed by using a projection algorithm (Kaufmann *et al.* 2008). The number of Stokes, ranging from 0.03 to 10, was computed over a "large" timescale of the turbulence seen by the particles, estimated by evoking the Tchen equilibrium in the spanwise direction which remains mean-flow free (Simonin 1991); the Stokes numbers were estimated over y-planes parallel to the streamwise direction and the value associated to each simulation refers to that found at the periphery of jet. The so-called "periphery" of the jet is a portion of the slab of y-coordinate ~ 0.7 corresponding to the periphery at the initial time.

The slab corresponds to the dispersion of a particle-laden turbulent planar jet into a homogenous isotropic decaying turbulence. The simulation domain is a cube of length size 2π, with a mesh grid of 128^3 cells and periodic in boundary conditions. Within the slab, of $d/L_{box} = 0.25$ of width, particles are randomly embedded. Mean velocity of particles is imposed equal to that

7th International Conference on Multiphase Flow,
ICMF 2010, Tampa, FL, May 30 – June 4, 2010

of the gas at the initial time. The Navier-Stokes equations are integrated by using a third order Runge-Kutta time stepping and a sixth order compact finite difference scheme on a cartesian grid. Also the advancement in time of the Lagrangian tracking is ensured by a third order Runge-Kutta scheme. The interpolation of the turbulent fields at the particle location is performed by a third order Lagrange polynomial algorithm. Without gravity, for small heavy particles, Lagrangian equations governing the motion of each k-particle are (Maxey & Riley 1983):

$$\frac{\mathrm{d}\mathbf{x}_p^{(k)}}{\mathrm{d}t} = \mathbf{v}_p^{(k)}, \quad \frac{\mathrm{d}\mathbf{v}_p^{(k)}}{\mathrm{d}t} = -\frac{1}{\tau_p}\left(\mathbf{v}_p^{(k)} - \mathbf{u}_{f\mathbb{G}p}^{(k)}\right) \quad (7)$$

where $\mathbf{u}_{f\mathbb{G}p}^{(k)}$ is the undisturbed velocity of the gas at the particle centre location. The particle relaxation time τ_p is defined in the Stokes regime as:

$$\tau_p = \frac{\rho_p d_p^2}{18\mu_f} \quad (8)$$

where ρ_p is the particle density, d_p the particle diameter and μ_f the dynamic viscosity of the gas.

A priori testing

"Exact" Eulerian mesoscopic fields, obtained by Lagrangian simulations, are then used to *a priori* check models. The model accuracy is evaluated by means of correlation coefficients at scalar level. Correlation coefficients are computed as follows (Salvetti & Banerjee 1995):

$$c = \frac{< AB > - < A >< B >}{\sqrt{(< A^2 > - < A >^2)(< B^2 > - < B >^2)}} \quad (9)$$

where brackets denote averages over y-planes. The evaluated scalar quantity represents the dissipation, by shear, of the mean mesoscopic energy into the mean RUM kinetic energy and it is written, accounting for the sign, as follows:

$$< \tilde{n}_p \delta R^*_{p,ij} \frac{\partial \tilde{u}'_{p,i}}{\partial x_j} >= n_p < \delta R^*_{p,ij} \frac{\partial \tilde{u}'_{p,i}}{\partial x_j} >_p \quad (10)$$

where n_p is the mean particle number density and the operator $< . >_p$ denotes particle-density-weighted average (over planes); if a mean mesoscopic velocity is defined $\tilde{U}_{p,i} =< \tilde{u}_{p,i} >_p$, then the fluctuating component is the residual $\tilde{u}'_{p,i} = \tilde{u}_{p,i} - \tilde{U}_{p,i}$. Moreover, the p.d.f. of the scalar quantity is also evaluated. The p.d.f. is plotted including the magnitude ratio between exact and modeled averaged quantities; in this manner only the shape

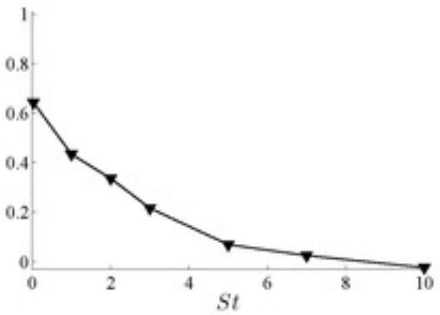

Figure 1: "VISCO" model (Eq. 4): correlation coefficients evaluated at scalar level over the mean dissipation (Eq. 10), at the periphery of jet.

is evaluated. The exact-to-modeled magnitude ratio represents a multiplicative coefficient which should be accounted for in order to predict the exact "mean" magnitude. This quantity is very important and it can seriously affect the success of the model if its value is far from one and it is not taken into account. Figure 1 shows correlation coefficients computed at the periphery of the jet, far from the start, for the model "VISCO". The model gives quite good correlations for small Stokes numbers while it fails when inertia increases. Looking at the p.d.f. of the mean dissipation (Figure 2), results show that the model is no able to reproduce positive values, meaning the local inverse transfer of energy from RUM to mesoscopic motion. This is a well-known limit of every viscosity-like model. Concerning the magnitude of modeled against exact dissipations, Figure 3 shows that such a model strongly overestimates the predictions; this behaviour is consistent with the re-laminarization of the dispersed phase observed by Riber (2007) when performing Eulerian-Eulerian simulations of the Hishida (1987) jet configuration. The overestimation increases with the particle inertia.

In order to supply an alternative to the model "VISCO", the structure of the deviatoric RUM ($\mathbf{R}^*$) and rate-of-strain ($\mathbf{S}^*$) tensors is analysed and information are used to construct new models.

The structure of the tensors

In order to study the structure of the tensors $\mathbf{R}^*$ and $\mathbf{S}^*$, since they are locally defined, we use a local dimensionless parameter proposed by Lund & Rogers (1994) and used by several authors involved in one-phase turbulent flow analysis (e.g., Tao *et al.* 2002, Higgins *et al.* 2003). This parameter, originally called "strain-state parameter" and used to study the "shape" of the defor-

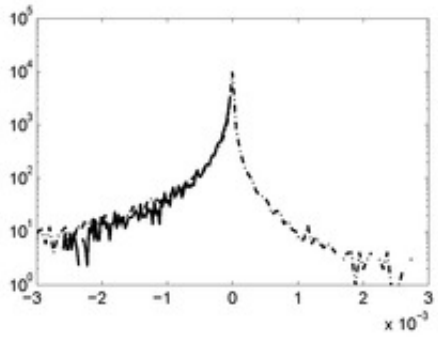

Figure 2: P.d.f. of the exact (dot-dashed line) against modeled by "VISCO" (solid line) local dissipation for simulation corresponding to $St \sim 1$, at the periphery of jet.

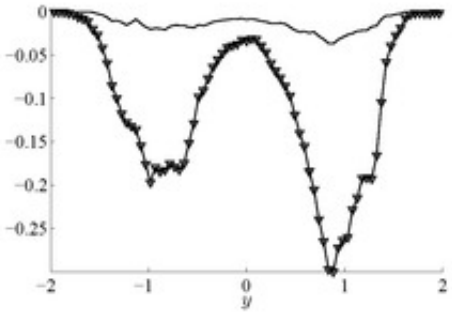

Figure 3: Profiles of exact (line) and modeled by "VISCO" (symbols) mean dissipations, for simulation corresponding to $St \sim 1$.

mations caused by the rate-of-strain tensor, may be used to investigate the structure of a traceless tensor giving local information about the relative magnitude of the tensor eigenvalues and reproducing information similarly to that found in the invariant Lumley's map. Hereinafter, the bold writing denotes second-rank tensors, brackets $\{.\}$ represents the trace and the asterisk means traceless when associated with a tensor. The dimensionless parameter is then defined as follows:

$$s^* = \frac{-3\sqrt{6}\,\lambda_1\,\lambda_2\,\lambda_3}{(\lambda_1^2+\lambda_2^2+\lambda_3^2)^{3/2}} \qquad (11)$$

where λ_1, λ_2 and λ_3 are the tensor eigenvalues. This parameter is bounded between $+1$ and -1 where $+1$ corresponds to an axisymmetric expansion and -1 is an axisymmetric contraction, in classical turbulence way of speaking. From a mathematical point of view $+1$ means that two identical eigenvalues dominate and that the third is small, while -1 means one large eigenvalue and the other two, identically small. For the sake of simplicity, we will use the same vocabulary than that used in turbulence, missing out, for the moment, any physical meaning. Figures 4 and 5 show the p.d.f. of s^* evaluated for both the deviatoric RUM and rate-of-strain tensors, for three different Stokes numbers and far from the initial time. Results show that the tensors $\mathbf{R}^*$ and $\mathbf{S}^*$ behave as in axisymmetric contraction and expansion respectively, independently from the inertia. Same results are found over all the planes of the jet. However, for large inertia and only at the periphery of the jet, the tensor $\mathbf{S}^*$ tends toward a more random distribution. Moreover, the

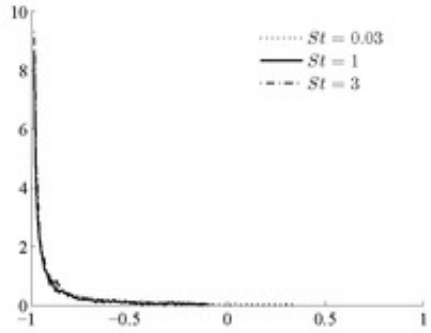

Figure 4: P.d.f.s of the parameter s^* evaluated for $\mathbf{R}^*$, at the periphery of jet.

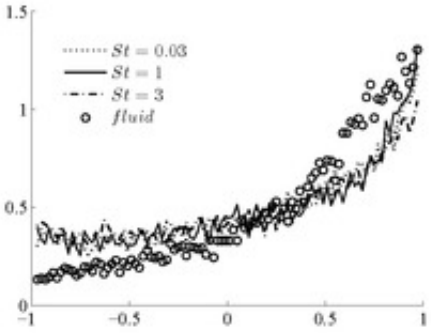

Figure 5: P.d.f.s of the parameter s^* evaluated for $\mathbf{S}^*$, at the periphery of jet. The rate-of-strain of the fluid is also evaluated.

analysis shows that the tensor $\mathbf{R}^*$ behaves as in one-component limit state, which means that the smallest eigenvalues of RUM tend to zero. This behaviour is developped immediately, in terms of time, in all the zones

of the jet, and it persists up to the end of each simulation for every Stokes number. In this case, theoretically, the eigenvalues are known. Indeed, following Lumley (1978), the eigenvalues of an averaged anisotropy tensor $\mathbf{g}^*$

$$\mathbf{g}^* = \frac{\mathbf{G}}{\{\mathbf{G}\}} - \frac{1}{3}\mathbf{I} = \frac{\mathbf{G}^*}{\{\mathbf{G}\}}, \tag{12}$$

corresponding to the one-component limit, are $\lambda_1 = \frac{2}{3}$, $\lambda_2 = \lambda_3 = -\frac{1}{3}$ in descending order. Consequently, the eigenvalues of the averaged tensor $\mathbf{G}$ or that of its deviatoric part $\mathbf{G}^*$ will be deducted (Simonsen & Krogstad 2005) via the relation

$$\lambda_{g_i^*} = \frac{\lambda_{G_i}}{\{\mathbf{G}\}} - \frac{1}{3} = \frac{\lambda_{G_i^*}}{\{\mathbf{G}\}}. \tag{13}$$

In the same way, but locally, we define the RUM anisotropy stress tensor as follows:

$$b^*_{p,ij} = \frac{\delta R_{p,ij}}{2\delta\theta_p} - \frac{1}{3}\delta_{ij} \tag{14}$$

for which the eigenvalues associated to the one-component-limit are known. Figure 6 shows the p.d.f. of the exact eigenvalues of $\mathbf{b}^*$ measured at the periphery of jet for a Stokes number close to one. The analysis shows that over all planes, for every Stokes number, the one-component limit state is reproduced. Hence,

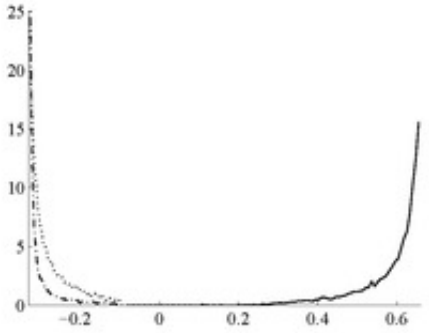

Figure 6: P.d.f.s of the eigenvalues of $\mathbf{b}^*$, at the periphery of the jet, for a simulation corresponding to $St \sim 1$.

the eigenvalues of the deviatoric tensor $\mathbf{R}^*$, sorted in descending order, are:

$$\mathbf{\Lambda}_{\mathbf{R}^*} \simeq \begin{pmatrix} +\frac{4}{3}\delta\theta_p & 0 & 0 \\ 0 & -\frac{2}{3}\delta\theta_p & 0 \\ 0 & 0 & -\frac{2}{3}\delta\theta_p \end{pmatrix}.$$

Modeling by using eigenvalues

In this section, information about the one-component limit state of the deviatoric RUM are used in order to suggest a new formulation of the stresses in function of the rate-of-strain tensor. This new formulation overcomes the problem of the tensor magnitude because it uses only information of the rate-of-strain principal directions assuming alignment between tensors.
As $\mathbf{R}^*$ and $\mathbf{S}^*$ are real and symmetric, then they always have an orthonormal basis composed by their real eigenvectors. Thus, in the principal axes, the assumption of the relative alignment of the two tensors may be traduced by the equality between their eigenvectors, being the magnitude taken into account by the respective eigenvalues. By using the linear transformation, the well-known relation may be used

$$\mathbf{R}^*\mathbf{x}_{\mathbf{R}^*} = \lambda_{R^*}\mathbf{x}_{\mathbf{R}^*} \tag{15}$$

where $\mathbf{x}_{\mathbf{R}^*}$ is a right column eigenvector of $\mathbf{R}^*$ and λ_{R^*} its correspondent eigenvalue. This relation may also be written in a matrix form as follows:

$$\mathbf{R}^*\mathbf{X}_{\mathbf{R}^*} = \mathbf{X}_{\mathbf{R}^*}\mathbf{\Lambda}_{\mathbf{R}^*} \tag{16}$$

where $\mathbf{X}_{\mathbf{R}^*}$ is the matrix of the tensor eigenvectors and $\mathbf{\Lambda}_{\mathbf{R}^*}$ is the diagonal matrix of the eigenvalues. As $\mathbf{R}^*$ and $\mathbf{\Lambda}_{\mathbf{R}^*}$ are similar matrix, $\mathbf{X}_{\mathbf{R}^*}$ is nonsingular, we may also write

$$\mathbf{R}^* = \mathbf{X}_{\mathbf{R}^*}\mathbf{\Lambda}_{\mathbf{R}^*}\mathbf{X}^{-1}_{\mathbf{R}^*}. \tag{17}$$

Then, using the assumption of alignment, which leads to $\mathbf{X}_{\mathbf{R}^*} = \mathbf{X}_{\mathbf{S}^*}$, the deviatoric RUM tensor can be straightforwardly obtained as follows:

$$\mathbf{R}^* = \mathbf{X}_{\mathbf{S}^*}\mathbf{\Lambda}_{\mathbf{R}^*}\mathbf{X}^{-1}_{\mathbf{S}^*} \tag{18}$$

where $\mathbf{\Lambda}_{\mathbf{R}^*}$ includes the known one-component limit eigenvalues. This model, referred to as "EIGEN", here evaluated by the *a priori* analysis, is instead less easy to handle when performing *a posteriori* Eulerian simulations because of the operation of matrix inversion and since it requires to initially check the right position of the deviatoric RUM eigenvalues into the matrix. In the next section another approach will be used leading to an equivalent formulation in Cartesian frame of reference.

A viscosity-type model for axisymmetric dispersed phases

In this section, the same procedure than in Jovanović *et al.* (2000) is applied. Following their idea for turbulent flows, tensors are assumed, as observed, axisymmetric

with the respect to a preferred direction and written in a bilinear form (Chandrasekhar 1950) leading to:

$$S^*_{p,ij} = A\delta_{ij} + B\lambda_i\lambda_j \tag{19}$$

$$\delta R^*_{p,ij} = C\delta_{ij} + D\lambda_i\lambda_j. \tag{20}$$

As the tensors are traceless, Eq. (19) and (20) can be rewritten as follows:

$$S^*_{p,ij} = A\delta_{ij} - 3A\lambda_i\lambda_j \tag{21}$$

$$\delta R^*_{p,ij} = C\delta_{ij} - 3C\lambda_i\lambda_j. \tag{22}$$

Defining the magnitude of the rate-of-strain tensor as the square-root of its second invariant $S = II_S^{1/2} = \{\mathbf{S^{*2}}\}^{1/2}$, Eq. (21), if contracted, makes it possible to obtain A as a function of S:

$$A = -sign(III_S)\frac{1}{2}\left(\frac{2}{3}\right)^{\frac{1}{2}} S \tag{23}$$

where $III_S = \{\mathbf{S^{*3}}\}$ is the third invariant of the tensor, and its sign accounts for the possibility to have an axisymmetric contraction or expansion. Eq. (21) then becomes:

$$S^*_{p,ij} = -sign(III_S)\left[\frac{1}{2}\left(\frac{2}{3}\right)^{1/2} S\delta_{ij} - \frac{3}{2}\left(\frac{2}{3}\right)^{1/2} S\lambda_i\lambda_j\right] \tag{24}$$

From Eq. (24), the product $\lambda_i\lambda_j$ may be expressed in function of the rate-of-strain:

$$\lambda_i\lambda_j = sign(III_S)\frac{2}{3}\left(\frac{3}{2}\right)^{1/2}\frac{S^*_{p,ij}}{S} + \frac{1}{3}\delta_{ij} \tag{25}$$

and injected into Eq. (22) wich takes the form:

$$\delta R^*_{p,ij} = -sign(III_S)3C\frac{2}{3}\left(\frac{3}{2}\right)^{1/2}\frac{S^*_{p,ij}}{S}. \tag{26}$$

The same relation may be provided for the anisotropy tensor

$$b^*_{ij} = -sign(III_S)\left[\frac{2}{3}\left(\frac{3}{2}\right)^{1/2}\frac{3C}{2\delta\theta_p}\frac{S^*_{p,ij}}{S}\right] \tag{27}$$

which contracted leads to the second invariant of the anisotropy II_b, from which we can obtain C as follows

$$C^2 = \frac{2}{3}II_b{\delta\theta_p}^2. \tag{28}$$

As well as for A, the sign of C is established by the sign of the third invariant III_b accounting for axisymmetric contraction or expansion

$$C = -sign(III_b)\left(\frac{2}{3}\right)^{1/2} II_b^{1/2}\delta\theta_p. \tag{29}$$

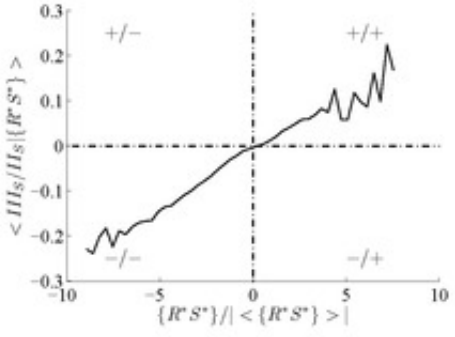

Figure 7: Conditional average of the normalized III_S over the normalized contracted product $R^*_{p,ij}S^*_{p,ij}$, for a simulation corresponding to $St \sim 1$, at the periphery of jet.

Including C into Eq. (26), we finally obtain

$$\delta R^*_{p,ij} = sign(III_S)sign(III_b)II_b^{1/2}2\delta\theta_p\frac{S^*_{p,ij}}{S}. \tag{30}$$

The product of the invariant signs accounts for the fact that the tensors may be both in the same configuration of "contraction" or "expansion" (positive sign) or in the opposite configuration (negative sign). Numerical simulations showed that the local sign of III_b is always positive ($\mathbf{b^*}$ is strictly in axisymmetric contraction) and only that of III_S changes. Moreover, numerical simulations pointed out the local one-component limit state of $\mathbf{b^*}$ which gives $II_b = \frac{2}{3}$. So, the model may be rewritten as:

$$\delta R^*_{p,ij} = sign(III_S)\left(\frac{2}{3}\right)^{1/2} 2\delta\theta_p\frac{S^*_{p,ij}}{S}. \tag{31}$$

The latter represents a model where the axisymmetry of tensors, their alignment, and the one-component limit state are assumed. Concerning the sign of the model, the sign of III_S is used to reproduce both positive and negative viscosities, i.e. negative and positive values of the contracted product $R^*_{p,ij}S^*_{p,ij}$, theoretically in that special case in which the axisymmetric rate-of-strain tensor moves from a configuration of expansion to contraction and vice versa. However, this assumption may be relaxed in practical applications. Figure 7 shows the conditional average of III_S over the contracted product $R^*_{p,ij}S^*_{p,ij}$ for a simulation corresponding to a number of Stokes $St \sim 1$. Results support such an assumption. Hereinafter, the model corresponding to Eq. (31) will refer to as "AXISY" model.

The relation between the model "EIGEN" and the model "AXISY" should be understood. The model "AX-

ISY" rewritten in terms of anisotropy leads to:

$$b^*_{p,ij} = sign(III_S)\left(\frac{2}{3}\right)^{1/2}\frac{S^*_{p,ij}}{S}. \qquad (32)$$

As $\mathbf{b}^*$ and $\mathbf{S}^*$ are real and symmetric, they may be written in the principal axes. Then, the assumption of the alignment, which leads to impose $\mathbf{X}_{\mathbf{b}^*}$=$\mathbf{X}_{\mathbf{S}^*}$, involves that also the eigenvalues are the same, of course accounting for every scalar included in the model. So, the expression for the eigenvalues becomes:

$$\lambda_i^{\mathbf{b}^*} = sign(III_S)\left(\frac{2}{3}\right)^{1/2}\frac{1}{S}\lambda_i^{\mathbf{S}^*}. \qquad (33)$$

Contracting the axisymmetric tensor $\mathbf{S}^*$, for instance when written in the configuration of expansion as follows

$$\begin{pmatrix} -2S_\lambda & 0 & 0 \\ 0 & S_\lambda & 0 \\ 0 & 0 & S_\lambda \end{pmatrix} \quad \begin{pmatrix} -2S_\lambda & 0 & 0 \\ 0 & S_\lambda & 0 \\ 0 & 0 & S_\lambda \end{pmatrix}$$

leads to write $S = \sqrt{6}S_\lambda$ where S_λ is the largest eigenvalue of $\mathbf{S}^*$. Including this relation into Eq. (33) and the right sign, gives:

$$\lambda_i^{\mathbf{b}^*} = -\frac{1}{3}\frac{\lambda_i^{\mathbf{S}^*}}{S_\lambda} \qquad (34)$$

which is fulfilled in our one-component limit state, giving evidence of the same model assumptions. Hence, theoretically, accounting for all the assumptions, using the model "EIGEN" is like to use the model "AXISY" in the principal directions. In practice, the two models can give different results. The models "EIGEN" and "AXISY" are viscosity-like models accounting for positive or negative local viscosity and using the timescale $\mathscr{F}(S^{-1})$ at the place of the particle relaxation time $\tilde{\tau}_p$ of the model "VISCO". Figure 8 shows correlation coefficients for all models evaluated over several simulations varying in Stokes number. Results for the models "EIGEN" and "AXISY" show a strongly improvement of predictions when compared with results of the model "VISCO". The ability of the new models to predict the reverse of sign is given by Figure 9 which shows the p.d.f. of the local dissipation evaluated by using the model "AXISY". Moreover, predictions of the mean dissipation magnitude are also improved, as shown by Figure 10 where the exact mean dissipation is compared to that modeled by using "VISCO" and "AXISY".

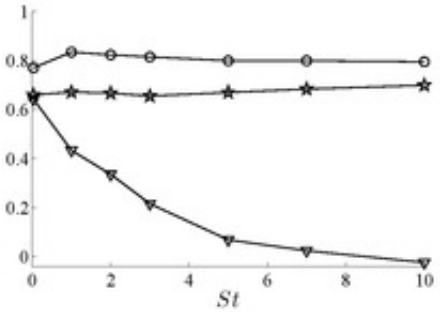

Figure 8: "VISCO" (triangles), "AXISY" (circles) and "EIGEN" (stars) models: correlation coefficients evaluated at scalar level for the mean dissipation (Eq. 10), at the periphery of jet.

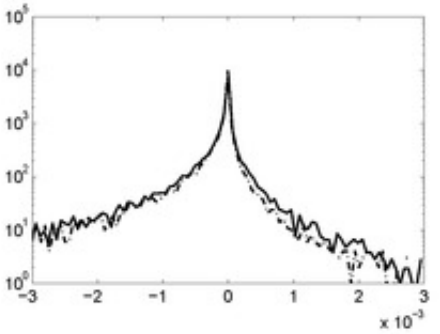

Figure 9: P.d.f. of the exact (dot-dashed line) against modeled by "AXISY" (solid line) local dissipation for simulation corresponding to $St \sim 1$, at the periphery of jet.

Conclusions and perspectives

In this paper the concern of the modeling of the second-order tensor accounting for in the momentum equation of the dispersed phase was addressed. An *a priori* study on a particle-laden turbulent planar jet, pointed out the inability of the viscosity model, commonly used, to predict such a tensor when the particle inertia increases. This model showed poor correlations at scalar level also overestimating the magnitude of the mean mesoscopic dissipation. An analysis of the tensor structure, including that of the rate-of-strain tensor, made it possible to characterize the "shape" of both the tensors. Tensors were found axisymmetric and the deviatoric RUM behaving as in a one-component limit state. Information of the tensor structure were then used for building alternative models. The linear viscosity-type models suggested in this paper strongly improve predictions of RUM stresses. A further study about nonlinear models is ongoing as well as preliminary *a posteriori* tests.

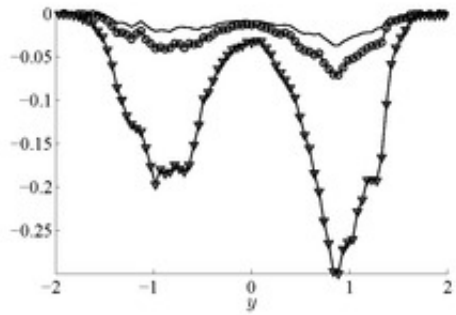

Figure 10: Profiles of exact (line) and modeled by "VISCO" (triangles) and "AXISY" (circles) mean dissipation, for simulation corresponding to $St \sim 1$.

Acknowledgements

This work received funding from the European Community through the TIMECOP-AE project (Project AST5-CT-2006-030828). It reflects only the author's views and the Community is not liable for any use that may be made of the information contained therein. Numerical simulations were performed by the IBM Power6 machine; support of Institut de Développment et des Ressources en Informatique Scientifique (IDRIS) is gratefully acknowledged.

References

Chandrasekhar S., The Theory of Axisymmetric Turbulence, Philosophical Transactions of the Royal Society of London, Series A, Mathematical and Physical Sciences, 242, n^o 855, pp.557-577, 1950

Février P., Simonin O. and Squires K.D., Partitioning of particle velocities in gas-solid turbulent flows into a continuous field and a spatially uncorrelated random distribution: theoretical formalism and numerical study, J. Fluid Mech., 533, pp.1-46, 2005

Higgins C.W., Parlange M., and Meneveau C., Alignment Trends of Velocity Gradients and Subgrid-Scale Fluxes in the Turbulent Atmospheric Boundary Layer, Boundary-Layer Meteorology, 109, pp.5983, 2003

Hishida K., Takemoto K. and Maeda M., Turbulent characteristics of gas-solids two-phase confined jet, Japanese Journal of Multiphase Flow 1, 1, pp. 5669, 1987

Jovanović J. and Otić I., On the Constitutive Relation for the Reynolds Stresses and the Prandtl-Kolmogorov Hypothesis of Effective Viscosity in Axisymmetric Strained Turbulence, Journal of fluids engineering, 122, pp. 48-50, 2000

Kaufmann A., Moreau M., Simonin O. and Helie J., Comparison between Lagrangian and Mesoscopic Eulerian Modeling Approaches for Inertial Particles Suspended in Decaying Isotropic Turbulence, J. Comp. Physics, 227, 13: 6448-6472, 2008

Lumley J.L., Computational Modeling of Turbulent Flows, Advances in applied mechanics, 18, pp. 123176, 1978

Lund, T. and Rogers M., An improved measure of strain state probability in turbulent flows, Phys. Fluids, 6 (5) , pp. 1838-1847, 1994

Maxey R. and Riley J., Equation of motion of a small rigid sphere in a nonuniform flow, Phys. Fluids, 26 (4), 883-889, 1983

Moreau M., Modélisation numérique directe et des grandes échelles des écoulements turbulents gaz-particules dans le formalisme eulérien mésoscopique, PhD thesis, INP Toulouse 2006, avalaible on the web site http://ethesis.inp-toulouse.fr/

Reeks M.W., On a kinetic equation for the transport of particles in turbulent flows, Phys. Fluids A 3, pp.446-456, 1991

Riber E., Modeling turbulent two-phase flows using Large-Eddy Simulation, PhD thesis, INP Toulouse 2007, avalaible on the web site http://ethesis.inp-toulouse.fr/

Salvetti M.V. and Banerjee S., A priori tests of a new dynamic subgrid-scale model for finite-difference large-eddy simulations, Phys. of Fluids, 7 (11), pp.2831-2847, 1995

Simonin O., Février P. and Laviéville J., On the spatial distribution of heavy-particles velocities in turbulent flow: from continuous field to particulate chaos, J. of Turb., 3, pp.1-18, 2002

Simonin O., Prediction of the dispersed phase turbulence in particulate laden jet, In Proc. 4th Int. Symp. on Gas-Solid lows, ASME-FED, 121, 197-206, 1991

Simonsen A.J. and Krogstad P.-A., Turbulent stress invariant analysis: Clarification of existing terminology, Phys. Fluids 17, 088103, pp.1-4, 2005

Tao B., Katz J. and Meneveau C., Statistical geometry of subgrid-scale stresses determined from holographic particle image velocimetry measurements, J. Fluid Mech., 457, 35-78, 2002